Materials Science-Poland, Vol. 26, No. 1, 2008

Computer simulation of tuned and detuned GaInNAsSb QW VCSELs for long-wavelength applications

K. GUTOWSKI, R. P. SARZAŁA*

Laboratory of Computer Physics, Institute of Physics, Technical University of Łódź, ul. Wólczańska 219, 93-005 Łódź, Poland

$Ga_{0.62}In_{0.38}N_{0.023}As_{0.95}Sb_{0.027}/GaN_{0.025}As_{0.975}$ quantum wells (QWs) used in standard GaAs-based GaInNAsSb/GaNAs vertical-cavity surface-emitting diode lasers (VCSELs) exhibit at room temperature (RT) the highest optical gain for the 1422 nm wavelength. Its RT continuous-wave threshold current for the 5 μm device is as low as only 0.68 mA. An increase in the QW active region temperature by about 100 K has been found to be followed by a shift of the gain spectrum of the above QW to the 1500 nm range. Therefore, a comprehensive computer simulation has been used to verify a possibility to highly detune GaAs-based GaInNAsSb/GaNAs VCSELs from the wavelength of 1422 nm to 1500 nm, closer to the wavelength used in the third generation of the fibre optical communication. Such a temperature-enhanced RT CW lasing operation of the 1500 nm VCSEL, with an active region identical to that of the 1422 nm one and the cavity properly re-designed for the 1500 nm wavelength, has been found to be reached at the threshold current as many as 17 times higher than that of the 1422 nm VCSEL.

Key words: *GaInNAsSb diode laser; 1.5 μm VCSELs; threshold laser simulation*

1. Introduction

Since discovering by Kondow et al. [1] unusual properties of GaInNAs, many research centres started investigations to manufacture diode lasers based on this material and exhibiting high performance in the 1.3 μm emission range. It has been later discovered that an addition of Sb not only enables producing quantum wells of higher quality without phase segregation and too many defects but it is also built-in into the chemical compound creating a new five-element GaInNAsSb compound [2–4] of even lower band-gap than GaInNAs [5]. This technology is still very immature and its properties are still not completely known. Therefore 1.5 μm RT continuous wave (CW) vertical cavity surface emitting diode lasers (VCSELs) have not been reported until now.

*Corresponding author, e-mail: rpsarzal@p.lodz.pl

The main goal of this work was to investigate properties of tuned and highly detuned GaInNAsSb VCSELs. Physical aspects of both a shift of the gain spectrum enhanced by an intentionally introduced active region temperature increase and a detuning of the VCSEL lasing emission following a cavity redesigning, from the 1422 nm radiation, corresponding to the room-temperature (RT) maximal optical gain of the GaInNAsSb QW, to the desired 1500 nm radiation have been analysed. The analysis is based on a modified version of the comprehensive three-dimensional optical-electrical-thermal-gain fully self-consistent VCSEL model which has been successfully used in our earlier simulations [6–9].

2. The model

Many VCSEL models have been reported in the literature. Their comparative analysis has been given by Osiński and Nakwaski [10] but none of them has been devoted to an advanced modelling of GaInNAsSb/GaNAs VCSELs. Recently, a comprehensive three-dimensional (3D) optical-electrical-thermal-gain self-consistent model of GaAs-based VCSELs has been developed to investigate their threshold RT operation. Both pulse and CW RT operations are considered. The model consists of four interrelated parts:

- The optical model describes, for successive radiation modes, their wavelengths and distributions of their optical fields within the resonator. The model is based on the effective frequency method [11]. The lasing threshold is determined from the condition of the real propagation constant.
- The finite-element (FE) electrical model characterizes both the current spreading (including carrier drift and diffusion processes) within the device volume between the top and the bottom contacts, the injection of both electrons and holes into the active region, their radial diffusion within it and their over-barrier leakage.
- The FE thermal model gives details of heat generation (non-radiative recombination, reabsorption of radiation as well as volume and barrier Joule heating) and its spreading from heat sources towards a heat sink and within it.
- The gain model, based on the Fermi golden rule, yields information about the optical gain spectra.

One of the important features of this well-conducted self-consistent approach is that it allows an integration of various physical phenomena, crucial for its RT CW operation, within a VCSEL device. The above means that all important, usually nonlinear, interactions between individual physical phenomena are taken into account using the self-consistent algorithm of calculations shown in Fig. 1. More details about the simulation model may be found elsewhere (cf. [5]). General rules of the advanced modelling of a VCSEL operation have also been formulated by Osiński and Nakwaski [10].

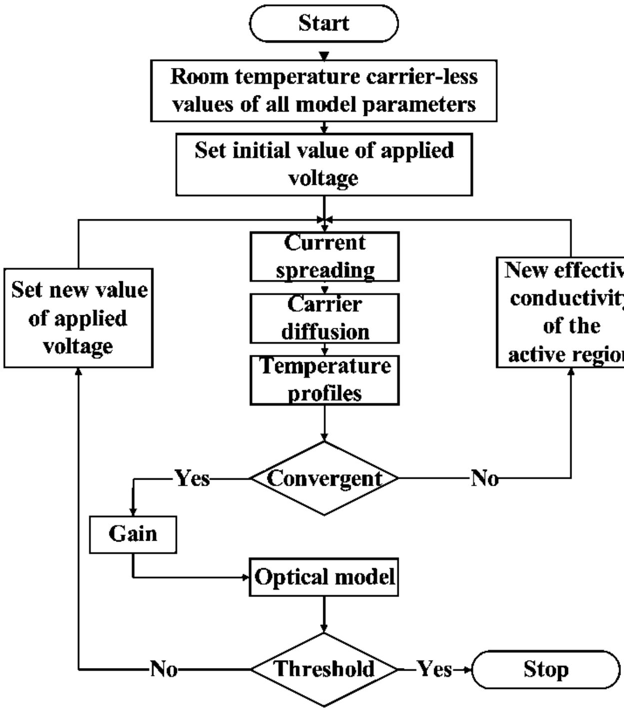

Fig. 1. Flow chart of the self-consistent calculation algorithm used in the modelling

3. The GaInNAsSb VCSEL structure

Let us consider the GaAs-based oxide-confined VCSEL configuration shown schematically in Fig. 2. Its active region is identical with that proposed by Goddard et al. [12]. Its modern double-intracavity-contact structure enables application of no-intentionally-doped distributed-Bragg-reflector (DBR) resonator mirrors which reduce optical absorption within them. The active region is a single 7.8 nm $Ga_{0.62}In_{0.38}N_{0.023}As_{0.95}Sb_{0.027}$ quantum well (QW) sandwiched by 22 nm $GaN_{0.025}As_{0.975}$ barriers.

To reduce the threshold current, the shortest possible (for the VCSEL configuration under consideration) 1.5λ cavity is assumed. 28 pairs of quarter-wave $Al_{0.8}Ga_{0.2}As$/GaAs layers and 34 pairs of AlAs/GaAs layers are used for the upper and bottom, DBRs respectively.The 15 nm central oxide aperture of the 5 μm diameter is created within the p-type spacer to create both electrical and optical radial confinements. The spacer parts neighbouring the active region are assumed not to be intentionally doped, whereas their parts important for radial current spreading from annular contacts towards centrally located active region are highly doped to enhance uniformity of carrier injection. The laser crystal is attached to the copper heat sink of a form of a cylinder of the 5 mm in diameter and 5 mm high.

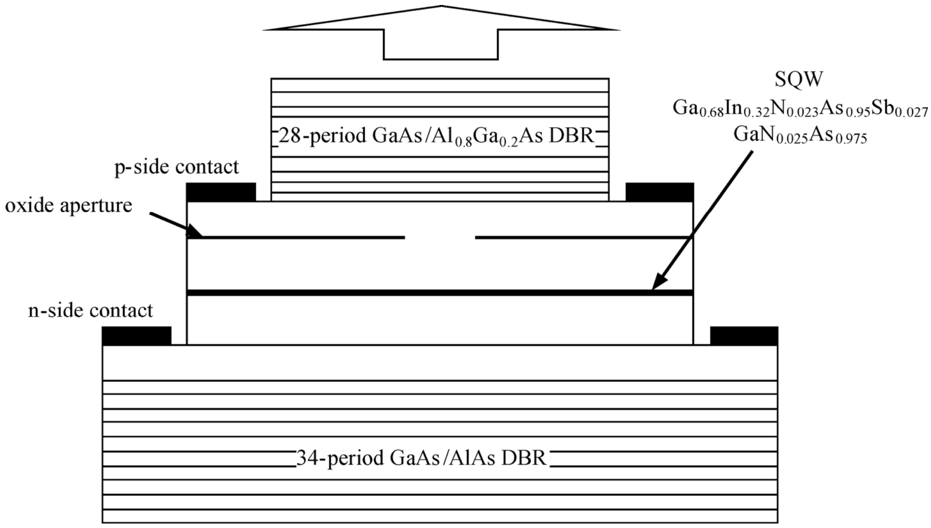

Fig. 2. The double-intracavity-contact GaAs-based oxide-confined GaInNAsSb/GaNAs quantum well vertical-cavity surface-emitting diode laser (VCSEL) structure

For a typical active region carrier concentration of 5×10^{18} cm^{-3}, the $Ga_{0.62}In_{0.38}N_{0.023}As_{0.95}Sb_{0.027}/GaN_{0.025}As_{0.975}$ QW active region has been found to exhibit the highest RT optical gain for the 1422 nm wavelength. Therefore, the reference VCSEL cavity has been designed for the same wavelength. To analyse a possibility to reach emission at longer wavelengths, the VCSEL cavity detuned for the 1500 nm emission has been additionally considered. For the both VCSEL designs, layer thicknesses are listed in Table 1.

Table 1. Layer thicknesses (in nm) in the 1422 nm and 1500 nm GaInNAsSb/GaNAs VCSELs

Layer	1422 nm VCSEL	1500 nm VCSEL
GaAs in bottom DBR	34×104.9	34×110.9
AlAs in bottom DBR	34×122.6	34×129.3
n-GaAs spacer (10^{18} cm^{-3})	100.0	100.0
n-GaAs spacer (10^{16} cm^{-3})	83.2	95.3
$GaN_{0.025}As_{0.975}$ barrier	22.0	22.0
$Ga_{0.62}In_{0.38}N_{0.023}As_{0.95}Sb_{0.027}$ QW	7.8	7.8
p-GaAs (10^{17} cm^{-3})	177.7	190.6
Al_xO_y	15.0	15.0
p-GaAs (2×10^{18} cm^{-3})	204.3	216.8
GaAs in upper DBR	28×104.9	28×110.9
$Al_{0.8}Ga_{0.2}As$ in upper DBR	28×118.9	28×125.8

4. Results

Radial profiles of the threshold current density j_{th} and the active region temperature T_A of the 1422 nm VCSEL operating at 300 K are shown in Fig. 3.

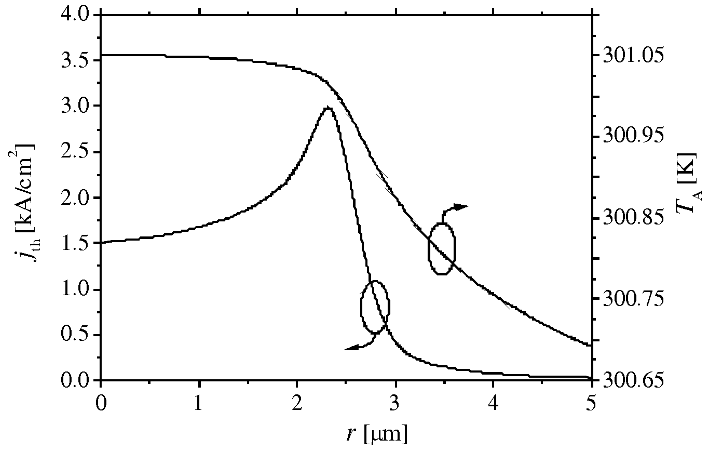

Fig. 3. Radial profiles of the threshold current density j_{th} and the active region temperature T_A of the 5 μm VCSEL emitting the 1422 nm radiation at 300 K

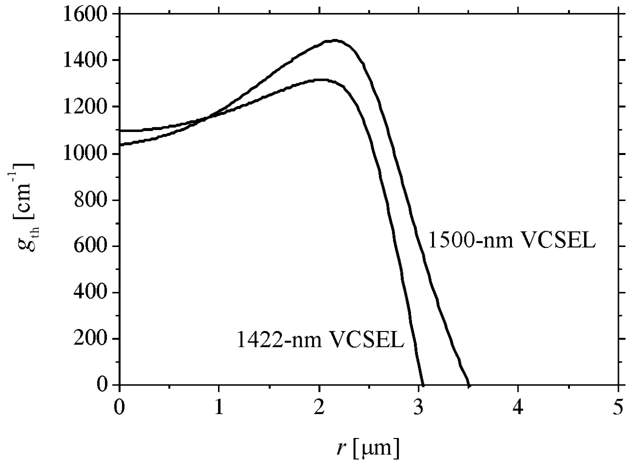

Fig. 4. RT radial profiles of the active region threshold optical gain g_{th} for the 5 μm VCSEL emitting the 1422 nm radiation and the 5 μm VCSEL emitting the1500 nm radiation

As one can see, current injection into the active region is in this case rather non-uniform with the current density close to the active region edge twice higher than that at the active region centre. This profile will be exchanged into somewhat less non-uniform threshold carrier concentration profile $n_{th}(r)$ because of radial diffusion of carriers within the active region before their recombination but the continually non-uniform radial gain profile (Fig. 4), roughly proportional to n_{th}, will be still unprofitable for the desired fundamental LP_{01} mode. Active region temperature is the highest at its centre and is rather slowly reduced within it and somewhat more speedily beyond it. Because of thermal focusing, it partially compensates the anti-guiding effect associated with the gain profile. Threshold operation parameters of the 5 μm VCSEL under consideration emitting 1422 nm radiation at 300 K are listed in Table 2.

Table 2. RT threshold operation parameters of the 5 μm VCSEL emitting the 1422 nm radiation and the 5 μm VCSEL emitting the 1500 nm radiation

I_{th} [mA]	$j_{\mathrm{th,max}}$ [kA/cm^2]	$g_{\mathrm{th,max}}$ [cm^{-1}]	$n_{\mathrm{th,max}}$ [10^{18} cm^{-3}]	$T_{A,\mathrm{max}}$ [K]	λ [nm]
5 μm VCSEL emitting the 1422 nm radiation					
0.68	3.04	1315	5.21	301.1	1422
5 μm VCSEL emitting the1500 nm radiation					
11.59	70.78	1487	17.25	393.7	1509

For the 1422 nm VCSEL, the relation of the threshold-current versus the maximum active region temperature is shown in Fig. 5. The lasing threshold has been found to strongly depend on temperature, which means that this VCSEL construction is very sensitive to changes of temperature. Accordingly, the characteristic temperature T_0 describing the above changes is equal to only 67.4 K for temperature increases not exceeding 55 K over the room temperature (RT = 300 K), whereas, for analogous GaInAs/GaAs VCSELs, it is as high as 160–200 K [9].

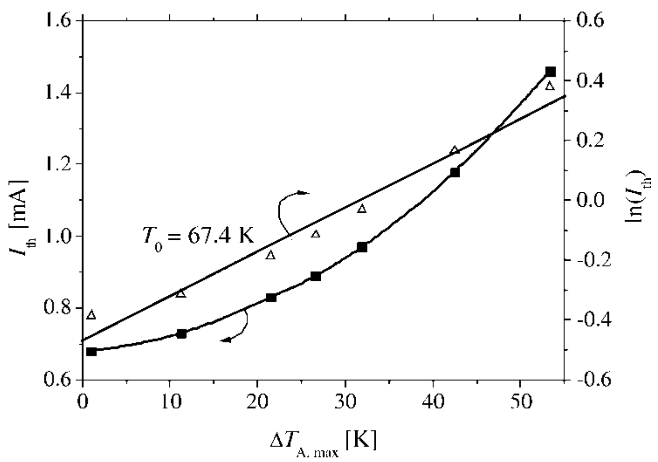

Fig. 5. Threshold current I_{th} of the 1422 nm VCSEL as a function of the maximum active region temperature increase $\Delta T_{A,\mathrm{max}}$ over 300 K (RT)

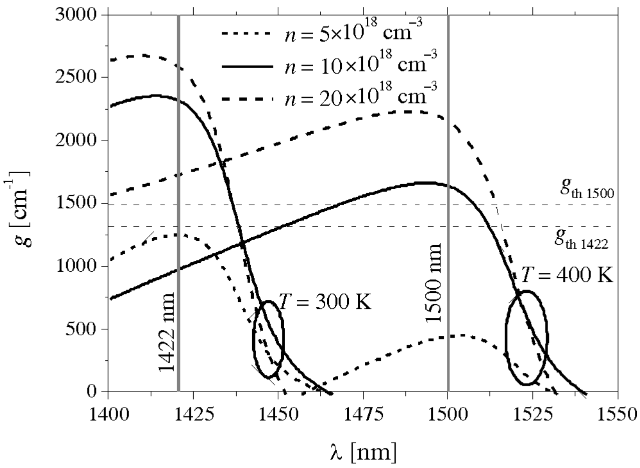

Fig. 6. The $Ga_{0.62}In_{0.32}N_{0.023}As_{0.950}Sb_{0.027}/GaN_{0.025}As_{0.975}$ quantum well gain spectra at 300 K and at 400 K for various active region carrier concentrations. Lasing thresholds for 1422 nm and 1500 nm are indicated

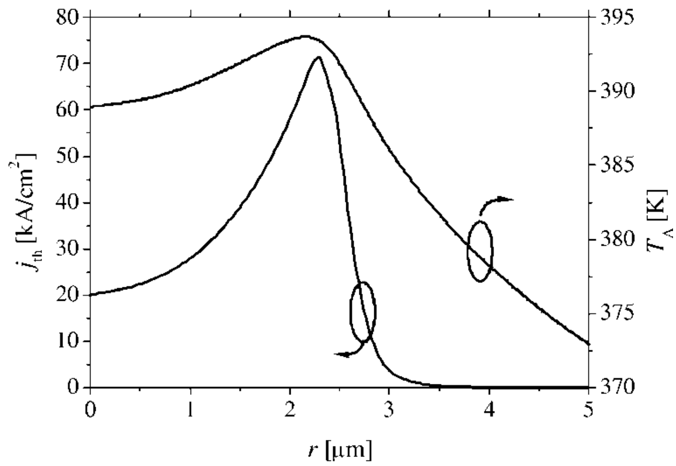

Fig. 7. Radial profiles of the threshold current density j_{th} and the active region temperature T_A of the 5 μm VCSEL emitting the 1509 nm radiation at 300 K

At RT, optical gain in the QW under consideration is limited to wavelengths shorter than 1465 nm even for very high carrier concentrations (Fig. 6). Then pulse currents of even very high amplitudes do not enable reaching the 1500 nm emission but at 400 K, QW gain spectra are found to be shifted to longer wavelengths and their maxima correspond to wavelengths close to 1500 nm. Because of heat generation close to the active region, such a temperature increase may be ensured by very high continuous wave (CW) operation currents. Then the threshold current at RT for the temperature enhanced 1500 nm emission of the VCSEL, with the same active region of diameter $\phi = 5$ μm but with the properly re-designed cavity (Table 1) will be as high as 11.59 mA (Table 2), which is as high as over 17 times greater than that for an analogous 1422 nm emission. Besides, current injection into the active region of the 1500 nm VCSEL (Fig. 7) has happened to be much more non-uniform than that of the 1422 nm VCSEL: its value close to the active region edge is over 3.5 times higher than that corresponding to the active region centre. Therefore radial threshold-gain profile is in this case considerably more non-uniform than in the case of the 1422 nm VCSEL (Fig. 4). Besides in the 1500 nm VCSEL, temperature is the highest close to the active region edge. Both the above profiles may enhance unwanted emission of the higher order LP modes.

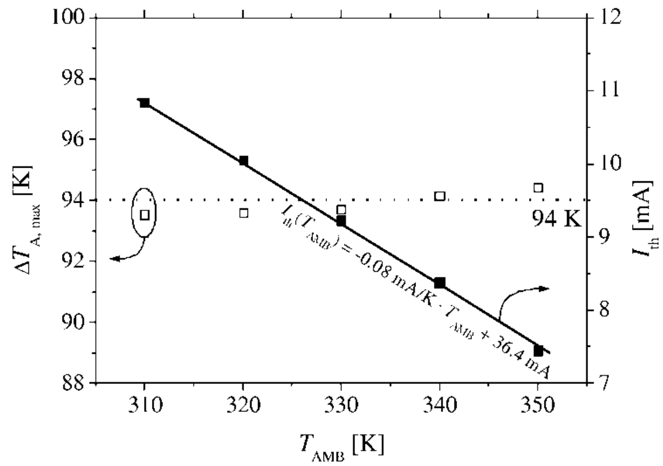

Fig. 8. Dependence on the ambient temperature T_{AMB} of the maximal active region temperature increase $\Delta T_{A,max}$ over RT and the threshold current I_{th} of the 5 μm VCSEL emitting the 1500 nm radiation

Active region temperature increase necessary to enhance the QW 1500 nm optical gain may also partly result from an increase in the ambient temperature T_{AMB} over RT. This is shown in Fig. 8 for the VCSEL re-designed for the 1500 nm emission (Table 1). For the lasing threshold, the maximum active region temperature increase over RT is nearly constant and equal to about 94 K disregarding the ambient temperature. On the opposite, the threshold current is steadily reduced for increasing T_{AMB}, because an additional current induced active region temperature increase necessary to shift the gain spectrum is gradually becoming lower.

5. Conclusions

Comprehensive computer simulation has been used to verify a possibility to highly detune GaAs-based GaInNAsSb/GaNAs QW VCSELs from the wavelength of

1422 nm, corresponding to the highest RT optical gain of its QW active region, to 1500 nm, closer to the wavelength used in the third generation of the fibre optical communication. Then the RT CW lasing operation of the 1500 nm VCSEL, with an identical active region to that of the 1422 nm one and the cavity properly re-designed for the 1500 nm wavelength (Table 1), may be reached for the active region temperature increased by about 94 K over RT which is necessary for a required QW gain shift to longer wavelengths. However, such a temperature induced CW RT VCSEL lasing operation at 1500 nm is reached for a threshold current as many as 17 times higher than that of the 1422 nm VCSEL.

References

[1] KONDOW M., UOMI K., NIWA A., KITATANI T., WATAHIKI S., YAZAWA Y., Jpn. J. Appl. Phys., 35 (1996), 1273.
[2] HA W., GAMBIN V., WISTEY M., BANK S., YUEN H., KIM S., HARRIS J.S., Electron. Lett., 38 (2002), 277.
[3] WISTEY M.A., *Growth of 1.5 μm vertical cavity surface emitting lasers by molecular beam epitaxy*, Doctoral Thesis, Stanford University (2005).
[4] VOLZ K., GAMBIN V., HA W., WISTEY M.A., YUEN H., BANK S., HARRIS J.S., J. Cryst. Growth, 251 (2003), 360.
[5] SARZAŁA R.P., NAKWASKI W., J. Phys.: Condens. Matter, 16 (2004), S3121.
[6] SARZAŁA R.P., MENDLA P., WASIAK M., MAĆKOWIAK P., BUGAJSKI M., NAKWASKI W., Opt. Quant. Electron., 36 (2004), 331.
[7] SARZAŁA R.P., IEEE J. Quant. Electron., 40 (2004), 629.
[8] SARZAŁA R.P., Semicond. Sci. Tech., 19 (2004), 1122.
[9] SARZAŁA R.P., *Diode Lasers for 2nd Generation of Fibre Optical Communication: Physical Simulation of an Operation and Optimization of Selected Laser Structure*, DSc Dissertation, Technical University of Łódź, Łódź, 2004
[10] OSIŃSKI M., NAKWASKI W., Chapter 5 [in:] *Vertical-Cavity Surface-Emitting Laser Devices*, Berlin, Springer, 2003, p. 135.
[11] WENZEL H.AND WÜNSCHE H.-J., IEEE J. Quant. Electron., 33 (1997), 1156.
[12] GODDARD L.L., BANK S.R., WISTEY M.A., YUEN H.B., EAO Z.L., HARRIS J.S., J. Appl. Phys., 97 (2005), 83101.

Received 28 April 2007
Revised 16 February 2008